Transient Concepts in Streaming Graphs

AIDA SHESHBOLOUKI and M. TAMER ÖZSU, University of Waterloo, Canada

Concept Drift (CD) occurs when a change in a hidden context can induce changes in a target concept. CD is a natural phenomenon in non-stationary settings such as data streams. Understanding, detection, and adaptation to CD in streaming data is (i) vital for effective and efficient analytics as reliable output depends on adaptation to fresh input, (ii) challenging as it requires efficient operations as well as effective performance evaluations, and (iii) impactful as it applies to a variety of use cases and is a crucial initial step for data management systems. Current works are mostly focused on passive CD detection as part of supervised adaptation, on independently generated data instances or graph snapshots, on target concepts as a function of data labels, on static data management, and on specific temporal order of data record. These methods do not always work. We revisit CD for the streaming graphs setting and introduce two first-of-its-kind frameworks *SGDD* and *SGDP* for streaming graph CD detection and prediction. Both frameworks discern the change of generative source. *SGDD* detects the CDs due to the changes of generative parameters with significant delays such that it is difficult to evaluate the performance, while *SGDP* predicts these CDs between 7374 to 0.19 milliseconds ahead of their occurrence, without accessing the payloads of data records.

CCS Concepts: • **Computer systems organization → Reliability**; • **Information systems → Data stream mining**.

Additional Key Words and Phrases: Concept Drift, Streaming Graphs

1 INTRODUCTION

Systems that run a data-driven decision making task (e.g., training/testing a learner model or answering a user-specified query), generate unreliable outputs when the input data or the decision factors are new, temporal, incomplete, or manipulated if the task does not recognize and manage it. A main cause identified for this problem is *concept drift* (CD) [17]. CD is a phenomenon that occurs when "changes in hidden context can induce more or less radical changes in target concept" [29]. Hidden context refers to insufficient, incomplete, or unobservable information about input data [6]. Target concept refers to known and/or observable information that have direct impact on the task's output. For instance, change of user opinions or customer relationship management affects the rating patterns; the data arrival from a certain location or type of users gets interrupted or changes, and this affects the distribution of arrivals; a mental health issue affects the driving patterns and generation of driving tickets or traffic control data; a biological function fluctuates the blood sugar level or heart beat rate; external factors deteriorate a wound tissue and the oxygen level drops and the temperature increases in the wound area.

In non-stationary settings such as that of streaming data, CD is natural [15, 19]. CD management covers three aspects [17]: CD detection to identify changes to characterize and quantify the drift; CD understanding to describe the drift event by providing information about the time, severity, and/or the contributing factors of drift; and CD adaptation to update a downstream task. Prompt CD management in streaming settings is important for generating relevant, reliable, and effective outputs. CD detection and understanding, our focus in this paper, benefit (i) development of accurate generative data models which are expected to (not) preserve concepts, (ii) generalization of analytics, (iii) designing algorithms (e.g., network protocols for error control and estimating the time-to-live of routing packets), and (iv) anomaly detections for "real-time monitoring or control of some automated activity", "organizing and personalizing information", and "characterizing health, well-being, or a state of humans, economics, or entities" [38].

In streaming data model, the streaming rate is highly dynamic and incurs simultaneous arrival of several bursts of data records, each generated at a time point. In applications where the payloads of data records are interconnected, it is helpful to model the data as a graph. The combination of

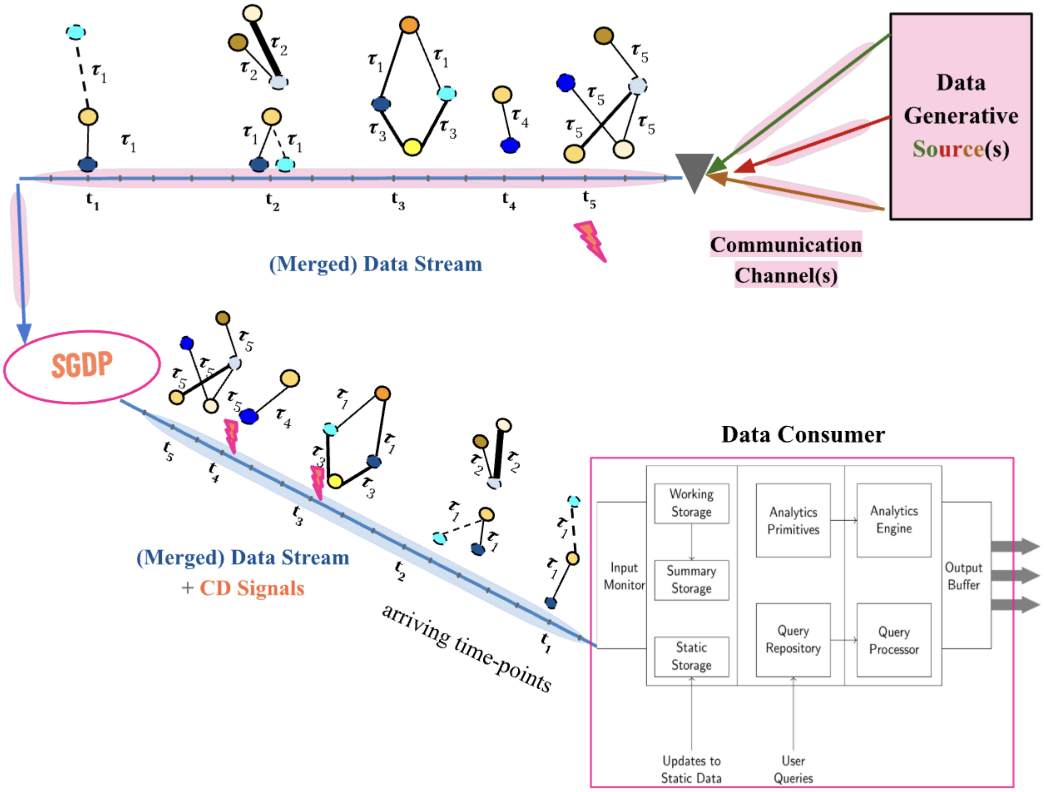

Fig. 1. Our CD Management scheme.

graph data and streaming leads to *streaming graphs*. Current CD management techniques do not consider this setting and generally incorporate a number of assumptions and design choices which do not always work properly due to the following.

a) The data is a sequence of totally ordered graph snapshots with vertex attributes and task labels [21, 33] and/or drift detection is integrated in online supervised systems, which means drifts are detected after one or more performance drops are observed in the data consumer task [8, 9, 13, 16, 28, 30, 36, 37]. The performance drop is associated to some sort of unidentified distribution change without proper justification [36, 37]. Another supervised CD detection method uses CD labels which differ from the labels of the consumer (task labels). These supervised settings are not always helpful:

* The drift signals cannot be used for other target tasks and the detection process should be repeated in a system performing multiple tasks on the same data (e.g., a large knowledge graph). The tasks may not require or use the same concepts and data labels.
* The task/CD labels and graph attributes are not always available due to privacy concerns, the cost of feature engineering, the cost of storing processed data, and the unknown nature of CD events, etc.
* While performance testing for CD detection runs, newly arrived data is processed or kept until the task is possibly updated. This delays the outputs and the CD signals can only help

with unprocessed data. Correcting the previous outputs and re-processing is expensive and not always feasible.

* The performance drop should not always be related to CD; e.g., the performance of a data model can decrease because the transductive model cannot be applied to new data, because the data is incomplete with missing representative samples or missing record elements, because the data is not clean, because the data is manipulated, etc.
* A performance drop caused by CD can be due to either a change in a data distribution (virtual CD) or a change in the relation between data and supervision labels (real CD). It is important to discern the CD type, which requires further computes.
* The performance of a data model does not necessarily drop or detect a CD. E.g., the model can be robust to CD, boosted by a CD , or miss a slow CD.
* Frequent performance checks can be wasteful when CDs are not frequent or abrupt.

b) The methods operate on streaming data records which are independently generated [15, 28, 36, 37] and compare the underlying distribution of sequential sets of data [5, 13]. Analyzing the payload of graph data records without considering the interconnectivity among them and their generation timestamps is not sound and complete.

* Using i.i.d. assumptions for graph edges which are not independently generated is misleading.
* The data records may arrive out-of-order or repeatedly; Using time-based sliding windows based on just arrival times or just generation timestamps would incur processing with incorrect temporal information.

c) The data is a sequence of windowed graphs or CD is detected using static parameters (e.g., a drift threshold, prototype baselines, window size, and slide size) [2, 13, 20, 21, 31, 31, 33, 36, 37]. Analyzing streaming edges with fixed parameters is not effective enough.

* Fixed drift thresholds cannot adapt to new concepts.
* Fixing the window (graph snapshot) sizes to static numbers is neither efficient nor effective with the highly dynamic streaming rates.
* An edge stream can be a mix of several streams generated by several sources and differentiating streams could incur additional costs (e.g., to separate the arrivals at one processing node). Graph streams commonly do not capture this heterogeneity.
* Evaluating the performance of batched analyses on graph streams is challenging. Accuracy can be influenced by the batch size. When several changes occur sequentially and the detection algorithm relies on historical information, a large batch and consequently a large system state, delays the detection outcomes, exhausts the memory, and the late detections can be viewed as missed/incorrect detections.

We revisit the transient concepts in streaming graphs to solve this problem: *Given the unbounded sub-sequence of streaming graph records, which are captured after a certain start point and partially ordered by their arrival time, how to signal a CD, while providing descriptive information about the drift without using supervision data labels.* We focus on the generative source as the hidden context (i.e., we signal the changes in the generative source(s) of streaming graph records) and do not consider factors such as merging, and sampling.

we define CD in streaming graphs as a change in a characteristic data pattern. We reduce the problem of CD signaling in streaming graphs to change detection in time-series of major data patterns. We choose data patterns that reflect the generative patterns of butterflies ((2,2)-bicliques) since (i) the streaming graph record (SGR)s in many applications capture the interactions that naturally occur in a bipartite mode, (ii) all complex networks have an underlying bipartite structure driving the topological structure of the unipartite version [12], (iii) butterflies are characteristic substructures in bipartite streaming graphs [25, 26], and (iv) butterflies can be listed incrementally without re-examining their existence.[1]

We introduce two frameworks: *SGDD*, for streaming graph drift detection via tracking the interconnectivity of butterflies, which serves as a baseline for an advanced framework *SGDP*, for streaming graph drift prediction via tracking the burstiness of the streaming edges. Both frameworks support any downstream analytics (supervised or unsupervised), explain the time and location of drifts, are unsupervised, adapt to the streaming rate, and do not require any input parameter. *SGDP* advances *SGDD* as it predicts CDs without utilizing data payloads (lightweight computations, privacy-preserving, and applicable to any data stream).

We demonstrate *SGDP* with the following motivating example. Figure 1 shows a sequence of SGRs (each with a generation timestamp τ_i and a non-empty payload) generated by one or more sources; Each SGR arrives at the data consumer at a time point t_j. The data records with the generation timestamp τ_5 and arrival time point t_5 are impacted by CD (a change in a hidden context e.g., an error in the transmission channel, a man-in-the-middle attack, a change of generative process or its parameters). *SGDP* receives the SGRs and at t_3 and t_4, CD signals are streamed out (before the arrival of impacted data records at t_5). *SGDP* monitors data patterns **without accessing the SGR payloads**. Moreover, it does not change the distribution of data arriving at the consumer system; it can and should be implemented in the input buffer of the consumer system for comprehensive CD checks or as a middleware exposed to further CDs. The CD signals can be incorporated in networking protocols (e.g., flipping a bit in the packet header with encryptions, sending a separate control packet, or watermark data annotation) – the specific implementation and notification methods are beyond the scope of this paper. The data consumer ingests the data records and the CD signals, and activates appropriate CD adaptation mechanisms (e.g., regulating the ingestion, data cleaning, updating the operators/storage/primitives/results, pushing forward the CD alerts as detected anomalies, etc).

Section 2 is a dictionary of terminology and notations. Section 3 reviews the methods on CD management. Sections 4 introduces *SGDP*. Section 5 introduces *SGDD* (details in Appendices A) and includes the performance evaluations. Section 6 concludes the paper.

2 DICTIONARY

1 (Streaming Record (SR), r_m). *A 2-tuple r_m=$\langle p, \tau\rangle$ where p defines the payload of the record and τ is its event (application) timestamp assigned by the data source. m is the record's index.*

2 (Streaming Graph Record (SGR), r_m). *A SR denoted as a quadruple r_m=$\langle i, j, \omega, \tau\rangle$, where the payload $p = \langle i, j, \omega\rangle$ indicates an edge with weight ω between vertices i and j.*

The payload can also include an operation such as add (solid edges in Figure 1) or delete (dashed edges in Figure 1). For simplicity, we assume all edges are added to the graph and do not consider the operation.

3 (Streaming Graph, $\mathfrak{R}$). *An unbounded sequence of SGRs denoted as $\mathfrak{R}$=$\langle r_1, r_2, \cdots\rangle$ in which each record r_m arrives at a destination unit at a particular time t_m ($t_m \leq t_n$ for $m<n$).*

4 (Burst, b). *A batch of S[G]Rs with the same timestamp and the same arrival time. b=$\{r_m \mid \nexists r_n : \tau_m = \tau_n, t_m = t_n, r_n \notin b\}$.*

We define a burst as the batch of records with the same timestamp which arrive at the computational system *together*. We do not define it as the *all SGRs* with the same timestamp, since payloads,

[1] Maximal subgraphs including several butterflies such as k-bitruss [27], k-wing [23], and $s(\alpha, \beta)_\tau$−core [14]) require dynamic maintenance.

timestamps, arrival time points of SGRs, or all of these (i.e., one or more co-arriving SGRs) can be repeated over time due to multiple generative sources and transmission issues. We order the SGRs by both arrival times and generation timestamps. This identifies late arrivals and enables defining a stream as a sequence of arriving bursts, regardless of processing/ingestion window. Figure 1 illustrates a stream with 15 SGRs arriving at 5 time-points leading to 7 bursts:

b_1=$\{r_1$=(p_1, τ_1), r_2=$(p_2, \tau_1)\}$, t_1
b_2=$\{r_3 = (p_3, \tau_2)$, r_4=$(p_4, \tau_2)\}$, b_3=$\{r_5$=(p_1, τ_1), r_6=$(p_2, \tau_1)\}$, t_2
b_4=$\{r_7 = (p_5, \tau_3)$, r_8=$(p_6, \tau_3)\}$, b_5=$\{r_9$=(p_7, τ_1), r_{10}=$(p_8, \tau_1)\}$, t_3
b_6=$\{r_{11}$=$(p_9, \tau_4)\}$, t_4
b_7=$\{r_{12}$=(p_3, τ_5), r_{13}=(p_{10}, τ_5), r_{14}=(p_{11}, τ_5), r_{15}=$(p_{12}, \tau_5)\}$, t_5

b_3 is the same as b_1, arriving at a later time-point. Also, b_5 has the same timestamp τ_1 as that of b_1 and b_3, since r_9 and r_{10} are late arrivals. Examples of these cases are when two sources concurrently send the same burst with the same generation time and one (b_3, b_5) arrives later, or when a networking protocol makes a duplicate (b_1) to compensate a delay.

Note, r_{15} denotes an edge with the same vertices as that of r_6, but with different weight; therefore, the payloads are different; Whereas, $r_{12} \in b_7$ repeats the payload of $r_3 \in b_2$, but not the timestamps. Therefore, these are not the same bursts.

5 (Window, W). *The set of SGRs within an specific interval.*

6 (Data Pattern, $\text{þ}(W)$). *A quantified data characteristic in a window. i.e.* $\text{þ}(W) : W \mapsto \mathbb{R}$.

7 (Transient Concept). *A non-stable data pattern in data records. i.e.* $\text{þ}(W) \mid \exists (W_1, t_1), (W_2, t_2) : \text{þ}(W_1) \neq \text{þ}(W_2)$.

8 (Concept Drift (CD)). *The event of a change in a transient concept.*

Considering a certain pattern þ, concept drift can be detected when observing at least two successive windows W_1 and W_2 corresponding to sequential time points t_1 and t_2, where $t_2 - t_1 \geq 1$ and $\text{þ}(W_1) \neq \text{þ}(W_2)$.

9 (Graph Snapshot, $G_{W,t}$). *The graph (V, E), formed at time point t by the vertices V and edges E of the SGRs within a corresponding window W.*

10 (Butterfly, $\bowtie^{i_1,i_2}_{j_1,j_2}$). *A $(2, 2)$-biclique between two i-vertices i_1, i_2 and two j-vertices j_1, j_2. It is a closed bipartite four-path* $\bowtie^{i_1,i_2}_{j_1,j_2} = \{i_1, j_1, i_2, j_2, i_1\}$.

11 (Young Butterfly, $\bowtie$). *A butterfly with j-vertices having a timestamp within the last x percentage of seen unique timestamps in the stream, i.e.* $\bowtie$=$\{\bowtie^{i_1,i_2}_{j_1,j_2} \mid \exists r_m, r_n : j_1 \in r_m, j_2 \in r_n, (\tau_m, \tau_n) \in [\tau_{t-\lceil xt \rceil}, \cdots, \tau_{t-1}, \tau_t]\}$.

Considering young butterflies (i.e. restricting the set of j-vertices), enables case studies where the freshness of input data is important and/or the goal is to perform processing over transient data records rather than all seen data records (streaming processing). This also accounts for the deletions in arriving *SGR*s. We set $x = 25\%$. Setting $x = 100\%$ would be equivalent to considering all seen vertices. The set of unique timestamps in the stream grows over time and consequently, the set of j-vertices within the x percentage grows. Choosing a low percentage helps to keep the size of this set balanced particularly when the streaming rate is high.

3 LITERATURE ON CD DETECTION

We review the CD management methods through the lens of a modular streaming framework [17] with three components: data management for retrieving and retaining data and system state in memory; drift detection for identifying changes and corresponding metadata; and drift adaptation for updating the downstream task. Accordingly, the existing works are divided in two groups: *active* (Figure 2) and *passive* (Figure 3). In active approaches, streaming data is continuously ingested and windowed via data management component and then drifts are explicitly detected and explained via drift detection component. This triggers updating the downstream task via drift adaptation. In passive approaches, a data model is learned in the data management component to extract the most important features of data for dimensionality reduction purposes, and the target goal of the downstream task. Based on the performance of this model (for instance, the learner's error), an implicit drift alert is signaled for drift adaptation. Since our focus is CD detection and understanding, we only review the data management and drift detection components of active and passive approaches. We refer the readers to comprehensive reviews of the works on drift adaptation [1, 10, 17]. We also do not review the line of works on anomaly detection (e.g. [7]). These works identify abnormal data records in known application contexts, while CD signaling is about identifying abnormal situations where a hidden contexts changes and data patterns including concepts change to some extend.

Data management. Data records are continuously ingested and windowed through the window management sub-component and possibly fed into a learner model through the data model sub-component (green boxes in Figures 2 and 3).

Window management. While in most passive approaches, a model is learned over a landmark window, active approaches usually use a two-window method with a *reference window* and a *data window*. Contents of data window are evaluated using the reference window as a baseline to determine whether a change has happened. While the data window covers the newly arrived data records, the reference window can be fixed [5, 18, 24] or moving [3, 15]. Some active approaches use single data window. Contents of each window instance are compressed to low dimensional embeddings. This results in a sequence of embeddings as the drift criterion [21, 31, 33]. Different techniques have been used for the window borders, window size, and sliding approach. Some approaches use landmark windows [9], while others use sliding windows [5, 13, 20, 21, 31, 33, 36, 37] with static time-based or count-based sizes [2, 5, 21, 31, 33] or dynamic sizes [4, 11]. When the window size is fixed, all/sampled streaming records are added/removed according to the size [21, 31, 33] or a weighting function is used to gradually remove elements with low weights [10].

Data model. In passive approaches, given a window, a data model is learned which performs the target adaptive task (green boxes in Figure 3). The decrease in model's effectiveness determines the need for an adaptation (yellow box in Figure 3). For instance, when the online error rate of a classifier reaches a drift threshold, a model update is required [8, 9, 13, 16, 30, 36, 37]. Some methods also consider a warning threshold to prepare a new model and replace it with the old model when the drift threshold is reached. Some methods involve a human to dismabiguate the drift type before drift adaptation [5].

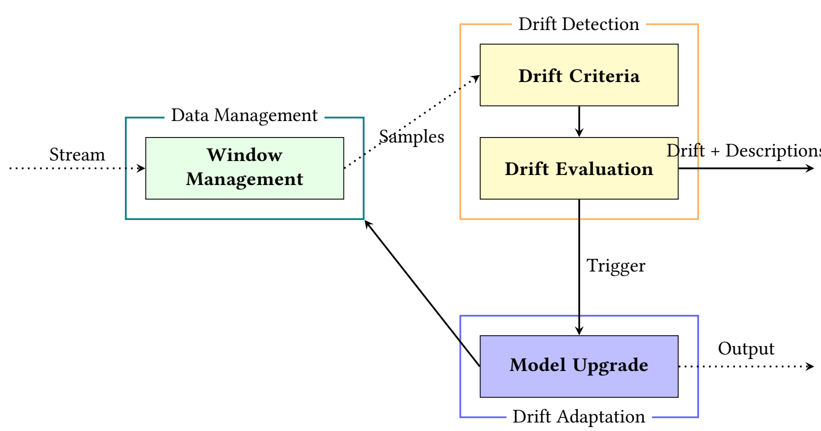

Fig. 2. Active concept drift management.

Drift detection. In active approaches, CD is usually detected when a statistical property of the data stream changes over time. The first formal definition of change detection in data streams [15] considers windows as data samples and computes their distribution distance to identify a drift using a hypothesis test method. This type of drift detection is also done using multiple hypothesis tests running in parallel or as a hierarchy of sequential tests [32, 35]. A recent line of research on graph streams (sequence of attributed or labeled graph snapshots) convert the graph stream to a time-series and perform change detection over it. The elements of

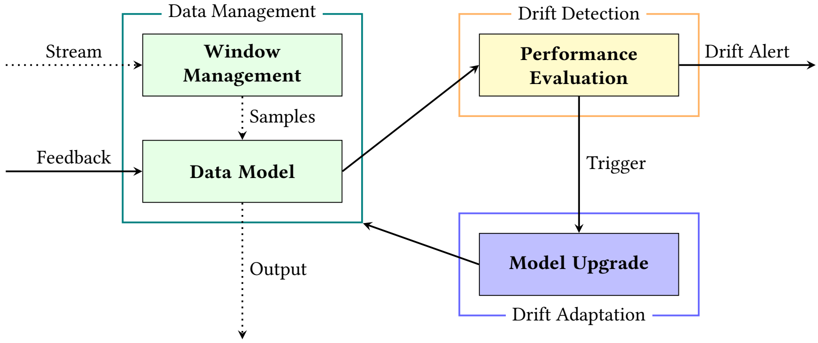

Fig. 3. Passive concept drift management.

time-series are prototype-based graph embedding vectors [33], or entropy of discriminative subgraphs with respect to classification labels [31] or with respect to a minimum description length [21]. The drift is evaluated by measuring a diversion dissimilarity [21] or a hypothesis test [33] and utilising a static threshold [21, 31, 33].

As we explain in the next sections, *SGDP* employs an active approach that extracts effective knowledge from the SGRs (the burstiness of the SGRs) on-the-fly, and efficiently maintain it as the system state. *SGDD* combines active and passive approaches and summarizes the stream into a graph of butterflies which is further reduced to two time-series (similarity of the butterfly neighborhoods and similarity of the future changes in butterfly neighborhoods) as the system state. Both *SGDP* and *SGDD* use a single data window and do not use reference window. The data window is a burst-based landmark window sliding with the arrival of each burst. In each window instance, the ingested timestamp of the newly arrived burst and the updated average burst size are captured in respective data collections. The SGR payloads are windowed in *SGDD* but not in *SGDP* and out-of-order timestamps are not captured repeatedly. *SGDP* and *SGDD* examine the time-series for CD signals. They both use dynamic thresholds set according to the number of detections and the streaming rate status.

4 SGDP

SGDP analyzes the time-series of burst sizes to signal an upcoming CD. This reduces the problem of CD signaling in streaming graphs to the problem of change detection in the time-series of burst sizes.

The functional architecture of *SGDP* is similar to that of active approaches (Figure 2). The main framework is given in Algorithm 1. *SGDP* performs two main tasks:

Data Management. This component extracts the burstiness properties of the stream and uses a sliding window with an adaptive length set to one burst, to append the current burst size to a time-series and regulate the frequency of analyses. *SGDP* just reads the generation timestamp of SGRs to extract and update the burstiness profile of the stream. It can even use a hash map of these timestamps. Hence, with minimum access to the data records and a light-weight time-series change detection, it predicts the change in the generative source of streaming (graph) data.

Drift Detection. The second component analyzes a suffix of the time series to check for upcoming CDs. Previous studies have shown that the characteristic substructure (butterflies) in streaming graphs emerge through bursty addition of edges to the graph [25, 26]. Therefore, *SGDP* detects a change in the burstiness patterns as an indication of abnormal generation processes. The frequency of these change detections depends on the streaming rate since the analyses start at the arrival of each burst (i.e., each window instance with a length adapting to the streaming rate).

4.1 SGDP - Data Management

The window management is done as follows.

Algorithm 1: SGDP()

Data: $\Re = \langle r_1, r_2, \cdots \rangle$, sequence of sgrs

1 $uniqueTimestamps \leftarrow \emptyset, W \leftarrow 1, t \leftarrow 1, B \leftarrow 1, \bar{B} \leftarrow 0, B_{max} \leftarrow 0, Bcount \leftarrow 0, \bar{B}series \leftarrow \emptyset,$ $W_d series \leftarrow \{0\}$
2 **while** $\exists r_t = \langle p_m, \tau_m \rangle$ **do**
3 $\quad Bcount \leftarrow uniqueTimestamps.size()$
4 $\quad$ **if** $uniqueTimestamps \ni \tau_t$ **then**
5 $\quad\quad B{+}{+}$
6 $\quad$ **else**
7 $\quad\quad \bar{B} \leftarrow (\bar{B} \times Bcount + B)/(|Bcount| + 1)$
8 $\quad\quad B \leftarrow 1$
9 $\quad$ **if** $B > B_{max}$ **then**
10 $\quad\quad B_{max} \leftarrow B$
11 $\quad\quad$ System.gc()
12 $\quad$ **if** $(\tau_t \notin uniqueTimestamps \;\&\; Bcount > 1)$ **then**
13 $\quad\quad \bar{B}series$.add($\bar{B}$)
14 $\quad\quad uniqueTimestamps.add(\tau_t)$
15 $\quad\quad$ **forall** $f \in \langle 1, 0.1, 0.9, 0.2, 0.8, 0.3, 0.7, 0.4, 0.6, 0.5 \rangle$ **do**
16 $\quad\quad\quad$ **if** $W - W_d series.lastElement() > \bar{B}$ **then**
17 $\quad\quad\quad\quad CDS_{Bursts}(B_{max}, \bar{B}, \bar{B}series, W, t, W_d series, f)$
18 $\quad\quad W{+}{+}$
19 $\quad$ **else**
20 $\quad\quad uniqueTimestamps.add(\tau_t)$
21 $\quad t{+}{+}$

1) When a SGR arrives, the burstiness profile of the stream is updated on the fly (Algorithm 1, Lines 3-11). This includes the number of seen bursts ($Bcount$), the size of current burst (B), the average burst size ($\bar{B}$), and the maximum seen burst size (B_{max}).

2) A new timestamp denotes a new burst (a new window instance with a dynamic size), which initiates CD check analysis over $\bar{B}series$ (Algorithm 1, Lines 12-18). The streaming rate of data records could be highly dynamic. While existing works disregard the generation timestamps of edges and analyze graph snapshots with a fix window size, *SGDP* uses burst-based windows with a size adapting to the burst sizes (streaming rate). We use this adaptive window length to resolve the following scalability problems of time-based windows with fixed sizes. When the streaming rate is high, either the window drops data records through sampling or sliding (trading the accuracy), or the window is split to sub-windows [34] and each sub-window is processed independently (losing the inter-connections among data or performing extra processing). E.g., consider a high degree vertex in a large graph with skewed degree distribution; where the neighbours of the vertex fall in disjoint sub-windows. Solving this issue requires further graph partitioning processes or double checking the connections between sub-windows, which defeats the efficiency purpose. When the rate is low, the window should wait for the arrival of data records to start the analyses (trading throughput).

When a new timestamp arrives, the updated average burst size is appended to a time series ($\bar{B}series$) and the timestamp is added to a hash set of unique values (Algorithm 1, Lines 13-14). If a repeated timestamp arrives (a late arrival), it would not be captured again.

3) Next, if the last CD signal has been in at least a distance of $\bar{B}$ previous windows, $\bar{B}series$ is analyzed for a CD signal at the current window (i.e., current burst). This analysis requires a threshold factor f. In our experiments we realized that most CD signals are issued when $f = 0.3$, therefore we just use this value. However other values can be tried for f (as suggested in Algorithm 1, Line 15).

4.2 SGDP - Drift Detection

CD check is done as follows:

1) To check for a CD signal, the last S elements of $\bar{B}serie$ are examined. This suffix size S increases as a function of the maximum and average burst sizes (Algorithm 2, Line 3).

2) If there are enough elements in $\bar{B}serie$, then the number of elements within the suffix that are greater and less than the current average burst size ($Ngreater$, $Nless$) are captured (Algorithm 2, Lines 6-11).

3) If any of these values passes a dynamic threshold ($\lceil S \times f \rceil$), a CD is signaled and the current window (burst) number is added to its corresponding time series $W_d series$ (Algorithm 2, Lines 14-15).

Algorithm 2: CD check via Burst sizes

1 **Function** $CDC_{Bursts}(B_{max}, \bar{B}, \bar{B}series, W, t, W_d series, f)$
2 $\quad d \leftarrow W_d series.size + 1$
3 $\quad S \leftarrow maxB^{\frac{\lfloor log_{10}(Max(maxB,100)) \rfloor}{\lfloor log_{10}(Max(\bar{B},10)) \rfloor}})$
4 $\quad s2 \leftarrow \bar{B}series.size(), Ngreater \leftarrow 0, Nless \leftarrow 0$
5 $\quad$ **if** $s2 > S$ **then**
6 $\quad\quad$ **forall** $i \leftarrow s2 - S - 1; i < s2; i{+}{+}$ **do**
7 $\quad\quad\quad temp \leftarrow \bar{B}series.elementAt(i)$
8 $\quad\quad\quad$ **if** $temp > \bar{B}$ **then**
9 $\quad\quad\quad\quad Ngreater{+}{+}$
10 $\quad\quad\quad$ **if** $temp < \bar{B}$ **then**
11 $\quad\quad\quad\quad Nless{+}{+}$
12 $\quad\quad threshold \leftarrow \lceil S \times f \rceil$
13 $\quad\quad$ **if** $Ngreater \geq threshold \bigvee Nless \geq threshold$ **then**
14 $\quad\quad\quad W_d series.add(W)$
15 $\quad\quad\quad$ Signal a drift at the sgr index t, window (burst) number W, and current system time

5 PERFORMANCE EVALUATION

Data. We simulate streaming graphs with ground truth about drift's time and pattern in the experiments. We synthesize 10^6 SGRs by the *sGrow* model [26], with a prefix of 1000 real-world SGRs from Amazon user-item stream[2]. *sGrow* as a configurable model generates bursts from several concurrent origins such that the streaming graph reproduces realistic subgraph emergence patterns. We simulate a change in a hidden context (change in the generative process) rather than a change in a target concept (e.g., subgraph inter-connectivity patterns). We refer to the switch from the 1000th real-world SGR to the first synthetic SGR as the first CD and simulate the next CDs as the following.

We introduce changes to the *sGrow*'s generative process via changing two parameters of *sGrow* which contribute the most to the emergence of butterflies: $[L_{min}, L_{max}]$ (range of preferential random walk's dynamic lengths), and ρ (burst connection probability). Two other parameters of the model (window parameter β and batch size M) are fixed. Parameters are set as the following:

- M and β can be set to any user-specified value without affecting the characteristic patterns of generated stream. we use the default values $\beta = 5$ and $M = 10$ in the experiments.
- The default value for ρ is 0.3 and for $[L_{min}, L_{max}]$ is $[1, 2]$. Increasing ρ to values less than 0.7 and expanding the range of $[L_{min}, L_{max}]$ ensure preserving butterfly emergence patterns, while decreasing the generation time and increasing burst size. We use $\rho = 0.4$ and $[L_{min}, L_{max}] = [1, 4]$ as the initial values to reduce the generation time while preserving realistic patterns and leaving room for drift simulation.

[2]Available at public repositories KONECT konect.uni-koblenz.de/networks/ and Netzschleuder networks.skewed.de

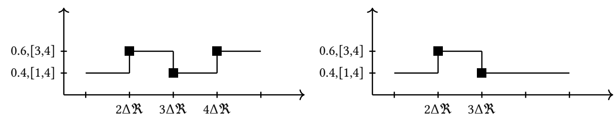

(a) Three changes for gradual CD (b) Two changes for recurring CD

Fig. 4. Evolution of *sGrow*'s parameters over the timeline of SGR generation. $\Delta\mathfrak{R} = 10^5, 2 \times 10^5$ is the drift interval in terms of the number of generated SGRs.

We simulate gradual and recurring drift patterns by switching the parameters of *sGrow* according to Figure 4. For gradual CD, the transient concept changes gradually and frequently, while spanning a considerable time interval until a new concept is stabilized. For recurring CD, the transient concept switches to a new concept and then it is repeated. We use drift intervals of $\Delta\mathfrak{R} = 10^5$ and 2×10^5 SGRs. We record the timestamp at which the drift is introduced for the evaluations.

Five stream instances are generated per pattern per drift interval for a total of 20 streams. We denote the streams as R_{ab} and G_{ab}, where

- R refers to recurring drifts.
- G refers to gradual drifts.
- $a = 1$ refers to $\Delta\mathfrak{R} = 1 \times 10^5$ (close-drift stream).
- $a = 2$ refers to $\Delta\mathfrak{R} = 2 \times 10^5$ (far-drift stream).
- $b \in \{1, 2, 3, 4, 5\}$ refers to the stream's instance number.

The length of the stream suffix without CD varies from $400K$ SGRs (R_{2b} and G_{2b}), to $600K$ SGRs (G_{1b}), and $700K$ SGRs (R_{1b}).

Metrics. CD signals are issued discretely. For each CD, we calculate the average system time distance (ms) and the SGR count distance between the CD and the first and last signals before that CD. The SGR count distance is fixed over multiple execution of the algorithms over a data stream, however the system time varies. We calculate the average time distances with 100 executions over each data stream since the standard deviation of the execution times is stabilized after 100 executions. We run the algorithm in 10 separate batch of 10 executions to overcome the caching/operating system effects on the performance.

Computing setup. We conduct the experiments with 15.6 GB native memory and Intel Core $i7{-}6770HQCPU@2.60GHz*$ 8 processor. All algorithms are implemented in Java (OpenJDK 17.0.12).

Baseline. Existing works on CD detection do not operate on streaming graphs, therefore we introduce a baseline framework, called *SGDD*, for streaming graph concept drift detection. *SGDD* represents the streaming graph as an evolving network of butterflies and tracks the similarity of neighbourhood of butterflies to signal CD. This reduces the problem of CD detection in bipartite streaming graphs to change detection in time series of similarity values.

SGDD's functional architecture is shown in Figure 5 and the main framework is given in Algorithm 3. *SGDD* performs two main tasks combining the architectures of active and passive approaches. Detailed descriptions are provided in Appendices A.1 and A.2.

Data Management. The goal is efficiently extracting and maintaining the state of the transient concept in the streaming graph (butterfly interconnectivity patterns). To this end, SGRs are ingested from the **b**ipartite streaming **g**raph to a burst-based sliding window W_{BG} and the burstiness profile of the stream is updated on the fly. At the arrival of each burst, W_{BG} is projected to a predicate-based sliding window W_{UWGO} which contains a **u**nipartite **w**eighted **g**raph of **o**scillators. Each vertex in UWGO is an oscillator and represents a young butterfly in W_{BG} with an oscillating phase denoting the butterfly's dynamic neighbourhood. The edge weights denote the neighbourhood sizes at the time of establishing connections among incident butterflies. The intuition is that the neighbourhood of a butterfly fluctuates between zero to $N - 1$ neighbours (where N is the number of butterflies in UWGO). Therefore, a butterfly's neighbourhood is represented by an oscillating

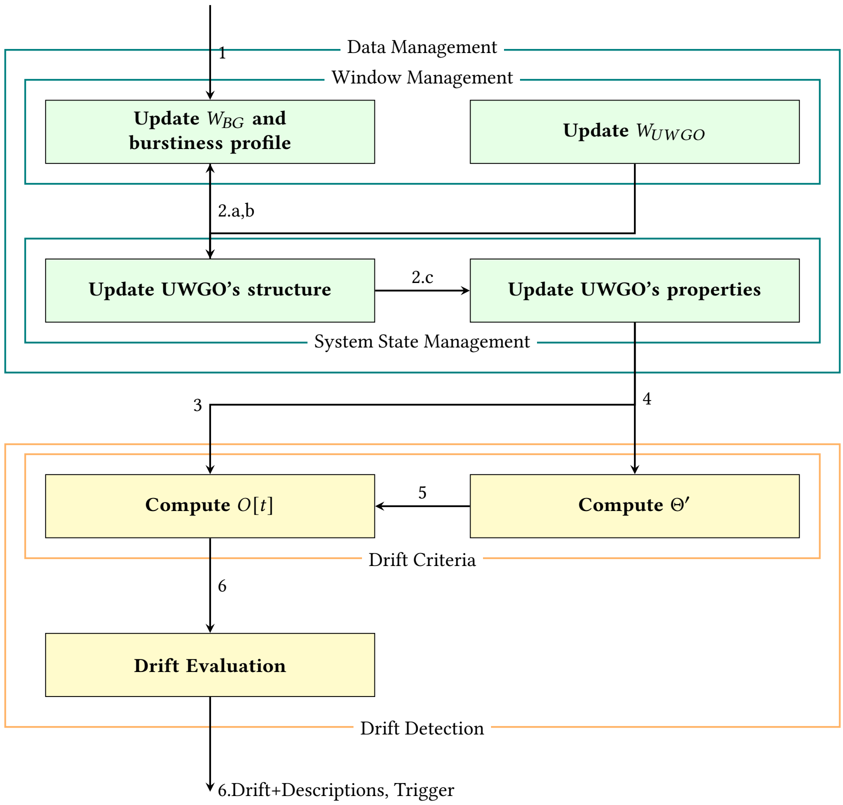

Fig. 5. *SGDD*'s architecture.

phase with a frequency of oscillation. Same butterfly neighbourhoods are hashed to the same phase. Therefore, $UWGO$ summarizes the interconnectivity of butterfly motifs in the original streaming graph (transient concept). W_{UWGO} has low computational overhead since it is updated incrementally. Moreover, W_{BG} is entirely retired as soon as it is projected to W_{UWGO} (i.e. it is a tumbling window). This (a) frees up memory for the drift detection since deleted objects are collected by the garbage collector and (b) avoids redundancy since in the next instance of W_{BG}, there wouldn't be any existing butterfly to be enumerated again. Also, W_{BG} and W_{UWGO} adapt to the streaming rate by adjusting the slide size to the burst sizes.

Drift Detection . A drift is detected by detecting a change in the drift criteria. The degree of global synchronization of phases in UWGO (similarity of butterfly neighbourhoods) reflects the density of butterfly interconnections (the relative size of the largest complete subgraph), and a change in the emergence of butterfly motifs indicates a change in the generative source(s) of the stream. Therefore, we analyze the synchronization of phases as a drift criterion. The challenge is that when the generative source changes, it takes a while for butterflies to form and connect according to the new generative condition and consequently the transient concept (UWGO) displays one or scattered changes with a delay. Therefore, just relying on the currently observed state of the transient concept and reporting a CD at the observation of a change in the synchronization would create false, duplicate, and delayed CD detections, while we want to signal each drift as soon as possible. To address this, we predict phase changes and analyze the synchronization of both the phases and their changes.

Table 1. The average system time distance (ms) / SGR count distance of the ith CD and its first and last SGDD's signals.

ms/SGR	d_{1f}	d_{1l}	d_{2f}	d_{2l}	d_{3f}	d_{3l}	d_{4f}	d_{4l}	d_{5f}	d_{5l}
G_{11}	1279.22/982	1279.22/982			875.45/19167	33.99/988	8537.4/98732	124.79/1864	51.4/876	22731.01/594829
G_{12}	1286.93/982	1286.93/982							224.74/2468	29664.04/597297
G_{13}	1318.93/982	1318.93/982							19796.47/208221	43807.36/596554
G_{14}	1305.08/982	1305.08/982							7467.8/87587	42014.77/600536
G_{15}	1316.48/982	1316.48/982			503.58/10751	0.35/233	8920.9/98988	115.65/1300	61.09/570	23105.18/594899
G_{21}	1345.31/982	1345.31/982			910.22/16152	188.32/4558	25925.09/198732	89.56/638	153.99/1843	25642.7/397538
G_{22}	1311.41/982	1311.41/982			4581.48/84374	65.07/921	22908.16/198384	64.05/505	172.88/2310	22775.03/399502
G_{23}	1381.85/982	1381.85/982			5327.45/134239	66.48/1825	16039.6/198208	0.9/721	207.83/4561	15697.04/395782
G_{24}	1324.19/982	1324.19/982			4879.08/105844	108.54/2335	20195.31/199897	182.62/2067	49.68/1236	20383.99/395417
G_{25}	1338.6/982	1338.6/982			4648.39/113738	25.84/2125	17670.39/197973	75.8/956	131.42/3098	17632.63/397629
AVG	1320.8/982	1320.8/982 /			3103.7/69180.7	69.8/1855	17171/170132	69.8/1150.1	2831.7/31277	26345.4/496998.3

ms/SGR	d_{1f}	d_{1l}	d_{2f}	d_{2l}	d_{3f}	d_{3l}	d_{4f}	d_{4l}
R_{11}	1475.07/982	1475.07/982					5935.04/57671	75446.28/600966
R_{12}	1447.28/982	1447.28/982					19451.59/158393	92599.45/664706
R_{13}	1539.74/982	1539.74/982					8017.77/71784	80846.53/602937
R_{14}	1332.92/982	1332.92/982					17077.71/146204	89826.2/686197
R_{15}	1418.04/982	1418.04/982			2849.95/68446	64.32/2566	105.79/1768	58976.76/596884
R_{21}	1381.17/982	1381.17/982	11046.09/98705	86.94/1267	9405.91/199209	106.17/3318	114.57/915	40008.31/398823
R_{22}	1376.46/982	1376.46/982			4329.28/66057	151.64/4311	128.32/893	44998.35/398598
R_{23}	1354.48/982	1354.48/982			6531.81/93877	223.41/4712	47.33/286	51448.63/398240
R_{24}	1349.71/982	1349.71/982					35030.2/222298	68710.73/399689
R_{25}	1348.72/982	1348.72/982			8990.3/103329	127.73/2970	124.7/675	55020.2/398164
AVG	1402.3/982	1402.3/982	11046.1/98705	86.9/1267	6421.4/106183.6	134.6/3575.4	8603.3 /66088.7	65788.1/514520.4

Table 2. The average system time distance (ms) / SGR count distance of the ith CD and its first and last *SGDP*'s signals : d_{if}, d_{il} in sGrow streams with gradual and recurring CD. The last two columns refer to the signals after the last CD.

ms/SGR	d_{1f}	d_{1l}	d_{2f}	d_{2l}	d_{3f}	d_{3l}	d_{4f}	d_{4l}	d_{5f}	d_{5l}
G_{11}	651.42/990	584.01/801	2762.67/197322	111.69/496	305.15/79689	8.51/23465				
G_{12}	683.68/990	607.8/801	3006.75/198233	1.32/3349	2463.45/91772	1933.86/25163	26.12/63150	5.67/13125		
G_{13}	609.44/990	535.87/801	1607.15/198294	0.96/2086	3150.85/95263	3.58/10180	39.02/98054	0.19/292	7.2/17716	1029.1/189478
G_{14}	598.39/990	534.11/801	2170.12/198157	1.99/5219	1758.48/98704	544.96/12354	33.05/95479	2.8/7674	2/5404	25.15/70548
G_{15}	648.8/990	575.54/801	3405/198337	1.13/2978	2272.32/86842	1056.86/58633				
G_{21}	566.15/990	484.24/801	2391.25/198283	1.08/2278	4687.6/193215	1389.33/32314				
G_{22}	641.91/990	572.85/801	2687.29/198289	2.46/7023	4017.14/196268	2293.06/111395				
G_{23}	631.01/990	553.63/801	3268.29/198489	1.12/3069	5695.47/184920	5695.47/184920				
G_{24}	656.74/990	586.69/801	3078.45/198172	1.11/3151	3758.52/190072	2739.9/147150				
G_{25}	717.63/990	639.03/801	3300.2/198171	1.64/4135	1683.72/187192	1675.52/164620				
AVG	640.52/990	567.38/801	2767.72/198174.7	12.45/3378.4	2979.27/140393.7	1734.1/77019.4	32.73/85561	2.89/7030.33	4.6/11560	527.12/130013

ms/SGR	d_{1f}	d_{1l}	d_{2f}	d_{2l}	d_{3f}	d_{3l}	d_{4f}	d_{4l}
R_{11}	636.49/990	558.96/801	2462.21/198127	2.45/6869	4278.58/97673	4278.58/97673	250.91/682266	250.91/682266
R_{12}	561.16/990	485.26/801	2409.21/198394	1.47/3558	976.68/94770	1.93/5188	3.11/9031	268.26/697540
R_{13}	542.94/990	472.12/801	2604.77/198448	0.6/1219	2217.9/86849	1084.84/31365	219.16/651394	233.98/691495
R_{14}	549.44/990	478.82/801	2796.4/198409	2.29/6153	3512.81/99174	1854.34/20925	21.43/63266	251.95/691375
R_{15}	637.72/990	560.35/801	3779.05/198169	3.08/8142	4835.85/93607	4835.85/93607		
R_{21}	699.96/990	615.46/801	5225.88/398443	5.35/13644	7374.02/195310	7374.02/195310		
R_{22}	630.29/990	558.23/801	3453.2/398254	2.2/4616	6982.72/192559	32.63/84623		
R_{23}	543.12/990	475.34/801	3502.31/398270	2.92/8113	3924.48/196196	1690.2/122332	130.03/384054	130.03/384054
R_{24}	544.31/990	474.32/801	2520.09/398463	1.87/4604	3696.13/196815	0.89/2159	4.31/11958	166.67/398053
R_{25}	539.37/990	471.82/801	3712.9/398096	1.1/2813	3373.39/186715	1212.24/114096	95.07/280736	135.51/383225
AVG	588.48/990	515.07/801	3246.6/298307.3	2.33/5973.1	4117.26/143966.8	2236.55/76727.8	103.43/297529.14	205.33/561144

Results. When the generative source of a streaming graph changes, *SGDD* signals CD with a notable delay especially when the change points are closer (R_{1b} and G_{1b} rows in Table 1). This delay is due to the time required for listing and analyzing butterflies and makes it difficult to distinguish the false positive signals (missed signals) and false negative signals (delayed signals). On the other hand, as shown in Table 2, *SGDP* discerns the synthetic SGRs from real-world SGRs (first CD) by issuing signals within SGR distance range of 990 – 810 and average system time distance of 640.52 – 567.38/588.48 – 515.07 (ms). Regarding the parameter changes, CD2 is approximately predicted between 3 seconds to 2 milliseconds before it occurs (198, 000 or 398, 0000 to variant numbers of SGRs). CD3 signals are issued from approximately 4 seconds until 2 seconds before it occurs (with different SGR distances across streams). And CD4 for G_{1b} streams is signaled from approximately 32 milliseconds until 2.89 milliseconds before its occurrence. False positive signals are more frequent for R_{ab} streams since the parameter drop leads to higher burst sizes making the CD checks analyzing a larger number of burst sizes due to the increase of maximum burst size and S, while the threshold increases. False negatives happen in G_{ab} streams only. We evaluated the performance of *SGDP* with the suffix size determined as $\frac{\lfloor log_{10}(Max(maxB,100))\rfloor}{\lfloor log_{10}(Max(\bar{B},10)\rfloor})^{(-1)^d}$ (Table 3). We observed this removal of the Maximum burst size from calculation for S, increases the false positives and also signals span almost the entire timeline of the SGR arrivals.

6 CONCLUSION

Concept drift is a natural phenomenon in streaming graphs. We define transient concepts and drift in streaming graphs. Our definitions enable studying diverse data patterns and concepts. We take the butterfly inter-connectivity patterns and introduce a framework for streaming graph drift detection, called *SGDD* which signals the drifts at the observation of butterfly neighbourhoods' tendency to change. *SGDD*'s data management techniques, which include identifying butterflies and the relative size of the largest complete network of butterflies, display promising visions for identifying maximal subgraphs and summarizing streaming graphs. We also focus on the burstiness characteristics of the stream and introduce an advanced framework for streaming graph drift *prediction*, called *SGDP*, which combines on-the-fly data management with minimum access to data records and light-weight drift prediction techniques. Both *SGDD* and *SGDP* can be integrated with any online adaptive analytics; they are designed as unsupervised techniques for understanding and detecting drifts in hidden contexts (generative sources) which are reflected in data patterns. While *SGDD* detects CDs with a delay, *SGDP* discerns the synthetic SGRs from real-world SGRs by issuing predictive signals within a distance range of 990 − 810 SGRs and average system time distance of 640.52 − 567.38 (ms) or 588.48 − 515.07 (ms). *SGDP* predicts parameter changes of the generative process(s) within a system time distance range of $\approx 4(s)$ to $\approx 2.89(ms)$ (starting at $\approx$ 198, 000 or 398, 0000 SGRs before the CD occurrence). *SGDP* can achieve false positives of zero in streams with gradual CD pattern. False negatives happen in streams with gradual CD patterns, but not in the streams with recurring CD pattern. Our experiments show this false positive/negative rates can be improved with further tuning the signaling algorithm.

REFERENCES

[1] Supriya Agrahari and Anil Kumar Singh. 2021. Concept Drift Detection in Data Stream Mining: A literature review. *Journal of King Saud University-Computer and Information Sciences* (2021).

[2] Brian Babcock, Shivnath Babu, Mayur Datar, Rajeev Motwani, and Jennifer Widom. 2002. Models and issues in data stream systems. In *Proc. 21st ACM SIGMOD-SIGACT-SIGART Symp. Principles of Database Systems.* 1–16.

[3] Stephen H Bach and Marcus A Maloof. 2008. Paired learners for concept drift. In *Proc. 8th IEEE Int. Conf. on Data Mining*. 23–32.

[4] Albert Bifet and Ricard Gavalda. 2007. Learning from time-changing data with adaptive windowing. In *Proc. 2007 SIAM Int. Conf. on Data Mining*. 443–448.

[5] Andrea Bontempelli, Fausto Giunchiglia, Andrea Passerini, and Stefano Teso. 2022. Human-in-the-loop handling of knowledge drift. *Data Mining and Knowledge Discovery* 36, 5 (2022), 1865–1884.

[6] Ryan Elwell and Robi Polikar. 2011. Incremental learning of concept drift in nonstationary environments. *IEEE Trans. Neural Networks* 22, 10 (2011), 1517–1531.

[7] Dhivya Eswaran, Christos Faloutsos, Sudipto Guha, and Nina Mishra. 2018. SpotLight: Detecting Anomalies in Streaming Graphs. In *Proc. 24th ACM SIGKDD Int.l Conf. on Knowledge Discovery & Data Mining*. 1378–1386.

[8] Isvani Frias-Blanco, José del Campo-Ávila, Gonzalo Ramos-Jimenez, Rafael Morales-Bueno, Agustin Ortiz-Diaz, and Yaile Caballero-Mota. 2014. Online and non-parametric drift detection methods based on Hoeffding's bounds. *IEEE Trans. Knowl. and Data Eng*. 27, 3 (2014), 810–823.

[9] Joao Gama, Pedro Medas, Gladys Castillo, and Pedro Rodrigues. 2004. Learning with drift detection. In *Proc. Brazilian Symp. on Artificial Intelligence*. 286–295.

[10] João Gama, Indrė Žliobaitė, Albert Bifet, Mykola Pechenizkiy, and Abdelhamid Bouchachia. 2014. A survey on concept drift adaptation. *ACM Comp. Surveys* 46, 4 (2014), 1–37.

[11] Heitor M Gomes, Albert Bifet, Jesse Read, Jean Paul Barddal, Fabrício Enembreck, Bernhard Pfharinger, Geoff Holmes, and Talel Abdessalem. 2017. Adaptive random forests for evolving data stream classification. *Machine Learning* 106, 9 (2017), 1469–1495.

[12] Jean-Loup Guillaume and Matthieu Latapy. 2004. Bipartite structure of all complex networks. *Inform. Process. Lett.* 90, 5 (2004), 215–221.

[13] Ben Halstead, Yun Sing Koh, Patricia Riddle, Russel Pears, Mykola Pechenizkiy, Albert Bifet, Gustavo Olivares, and Guy Coulson. 2022. Analyzing and repairing concept drift adaptation in data stream classification. *Machine Learning* 111, 10 (2022), 3489–3523.

[14] Yizhang He, Kai Wang, Wenjie Zhang, Xuemin Lin, and Ying Zhang. 2021. Exploring cohesive subgraphs with vertex engagement and tie strength in bipartite graphs. *Information Sciences* 572 (2021), 277–296.

[15] Daniel Kifer, Shai Ben-David, and Johannes Gehrke. 2004. Detecting change in data streams. In *Proc. 30th Int. Conf. on Very Large Data Bases*, Vol. 4. 180–191.

[16] Anjin Liu, Guangquan Zhang, and Jie Lu. 2017. Fuzzy time windowing for gradual concept drift adaptation. In *Proc. 2017 IEEE Int. Conf. on Fuzzy Systems*. 1–6.

[17] Jie Lu, Anjin Liu, Fan Dong, Feng Gu, João Gama, and Guangquan Zhang. 2019. Learning under Concept Drift: A Review. *IEEE Trans. Knowl. and Data Eng.* 31, 12 (2019), 2346–2363.

[18] Ning Lu, Guangquan Zhang, and Jie Lu. 2014. Concept drift detection via competence models. *Artificial Intelligence* 209 (2014), 11–28.

[19] Jose G Moreno-Torres, Troy Raeder, Rocío Alaiz-Rodríguez, Nitesh V Chawla, and Francisco Herrera. 2012. A unifying view on dataset shift in classification. *Pattern Recognition* 45, 1 (2012), 521–530.

[20] Kyosuke Nishida and Koichiro Yamauchi. 2007. Detecting concept drift using statistical testing. In *Proc. Int. Conf. on Discovery Science*. 264–269.

[21] Ramesh Paudel and William Eberle. 2020. An approach for concept drift detection in a graph stream using discriminative subgraphs. *ACM Transactions on Knowledge Discovery from Data* 14, 6 (2020), 1–25.

[22] Francisco A Rodrigues, Thomas K DM Peron, Peng Ji, and Jürgen Kurths. 2016. The Kuramoto model in complex networks. *Physics Reports* 610 (2016), 1–98.

[23] Ahmet Erdem Sarıyüce and Ali Pinar. 2018. Peeling bipartite networks for dense subgraph discovery. In *Proc. 11th ACM Int. Conf. Web Search and Data Mining*. 504–512.

[24] Junming Shao, Zahra Ahmadi, and Stefan Kramer. 2014. Prototype-based learning on concept-drifting data streams. In *Proc. 20th ACM SIGKDD Int. Conf. on Knowledge Discovery and Data Mining*. 412–421.

[25] Aida Sheshbolouki and M Tamer Özsu. 2022. sGrapp: Butterfly Approximation in Streaming Graphs. *ACM Trans. Knowledge Discovery from Data* 16, 4 (2022), 1–43.

[26] Aida Sheshbolouki and M. Tamer Özsu. 2023. sGrow: Explaining the Scale-Invariant Strength Assortativity of Streaming Butterflies. *ACM Transactions on the Web* 17, 3 (2023), 1–46.

[27] Kai Wang, Xuemin Lin, Lu Qin, Wenjie Zhang, and Ying Zhang. 2020. Efficient bitruss decomposition for large-scale bipartite graphs. 661–672.

[28] Scott Wares, John Isaacs, and Eyad Elyan. 2019. Data stream mining: methods and challenges for handling concept drift. *SN Applied Sciences* 1 (2019), 1–19.

[29] Gerhard Widmer and Miroslav Kubat. 1996. Learning in the presence of concept drift and hidden contexts. *Machine Learning* 23, 1 (1996), 69–101.

[30] Shuliang Xu and Junhong Wang. 2017. Dynamic extreme learning machine for data stream classification. *Neurocomputing* 238 (2017), 433–449.

[31] Yibo Yao and Lawrence B Holder. 2016. Detecting concept drift in classification over streaming graphs. In *Proc. KDD Workshop on Mining and Learning with Graphs*. 2134–42.

[32] Shujian Yu, Xiaoyang Wang, and José C Príncipe. 2018. Request-and-reverify: Hierarchical hypothesis testing for concept drift detection with expensive labels. *arXiv preprint arXiv:1806.10131* (2018).

[33] Daniele Zambon, Cesare Alippi, and Lorenzo Livi. 2018. Concept drift and anomaly detection in graph streams. *IEEE Trans. Neural Networks and Learning Systems* 29, 11 (2018), 5592–5605.

[34] Chao Zhang, Angela Bonifati, and M. Tamer Özsu. 2024. Incremental Sliding Window Connectivity over Streaming Graphs. *Proc. VLDB Endow.* 17, 10 (2024), 2473–2486.

[35] Yuhong Zhang, Guang Chu, Peipei Li, Xuegang Hu, and Xindong Wu. 2017. Three-layer concept drifting detection in text data streams. *Neurocomputing* 260 (2017), 393–403.

[36] Ming Zhou, Jie Lu, Pengqian Lu, and Guangquan Zhang. 2024. Dynamic Graph Regularization for Multi-Stream Concept Drift Self-adaptation. *IEEE Trans. Knowl. and Data Eng.* (2024).

[37] Ming Zhou, Jie Lu, Yiliao Song, and Guangquan Zhang. 2023. Multi-stream concept drift self-adaptation using graph neural network. *IEEE Trans. Knowl. and Data Eng.* 35, 12 (2023), 12828–12841.

[38] Indrė Žliobaitė, Mykola Pechenizkiy, and Joao Gama. 2016. An overview of concept drift applications. In *Big Data Analysis: New Algorithms for a New Society*, Nathalie Japkowicz and Jerzy Stefanowski (Eds.). 91–114.

A APPENDICES

A.1 SGDD - Data Management

The interleaved procedures of window management and system state management are as follows (steps 1 and 2 and green boxes in Figure 5).

Algorithm 3: SGDD()

Data: $\Re = \langle r_1, r_2, \cdots \rangle$, sequence of sgrs

1 $BBG \leftarrow \emptyset$, $UWGO = (V, E) \leftarrow \emptyset$, $uniqueTimestamps \leftarrow \emptyset$, $W \leftarrow 1$, $t \leftarrow 1$, $B \leftarrow 1$, $\bar{B} \leftarrow 0$, $maxB \leftarrow 0$, $Bcount \leftarrow 1$, $d \leftarrow 0$, $W_d serie \leftarrow \{0\}$

2 **while** $\exists r_t = \langle i_t, j_t, \omega_t, \tau_t \rangle)$ **do**

3     $Bcount \leftarrow uniqueTimestamps.size()$

4   **if** $uniqueTimestamps \ni \tau_t$ **then**

5         $B{+}{+}$

6   **else**

7         $\bar{B} \leftarrow (\bar{B} \times Bcount + B)/(|Bcount| + 1)$

8         $B \leftarrow 1$

9   **if** $B > B_{max}$ **then**

10         $B_{max} \leftarrow B$

11   System.gc()

12   **if** $BG \not\ni (i_t, j_t)$ **then**

13         $BG.addedge(i_t, j_t)$

14   **if** *(*$uniqueTimestamps \not\ni \tau_t$ & $Bcount > 1$*)* **then**

15         $uniqueTimestamps.add(\tau^t)$

16   Project BG to $UWGO$

17         $BG \leftarrow \emptyset$

18   **forall** $v \in V$ **do**

19             $\theta_v \leftarrow (\Sigma_{n \in N(v)} n.ID)\%2\pi$

20             $\Omega_v \leftarrow$ sample from a Gaussian distribution

21   System.gc()

22         $O_1[W] \leftarrow ((\sum_{v \in V} sin\theta_v)^2 + (\sum_{v \in V} cos\theta_v)^2)^{\frac{1}{2}}/|V|$

23         $\Delta\theta \leftarrow RungeKutta(UWGO, 0.01)$

24         $O_2[W] \leftarrow ((\sum_{v \in V} sin\Delta\theta_v)^2 + (\sum_{v \in V} cos\Delta\theta_v)^2)^{\frac{1}{2}}/|V|$

25         $CDC_{Butterfly}(\bar{B}, maxB, O_1, O_2, t, W, W_d serie)$

26         $W{+}{+}$

27   **else**

28         $uniqueTimestamps.add(\tau^t)$

29     $t{+}{+}$

1) Arriving SGRs are added to W_{BG} and the burstiness profile of the stream is updated online (Algorithm 3, lines 3-13). When one burst is seen, W_{BG} is closed and the following steps 2 to 7 are performed (Algorithm 3, lines 14-26).

2) W_{BG} is projected to update W_{UWGO}.

2.a) The UWGO structure is updated by identifying the young butterflies, mapping them to UWGO vertices, and connecting these vertices (Algorithm3, line 16 invoking Algorithm 4). The young butterflies are identified

Algorithm 4: Project W_{BG} to W_{UWGO}

forall $\bowtie_v = \{i_1, j_1, i_2, j_2, i_1\} \in BG$ **do**
  $v \leftarrow$ new UWGO vertex with $\theta_v = 0$, $\Omega_v = 0$, $ID = 0$
  $v.setID(v.hashCode())$
  $UWGO.add(v)$
  Add young butterflies adjacent to j_1 and j_2 to L
  forall $\bowtie_u \in L$ **do**
    $UWGO.addEdge(u, v, |L|)$
Local data structures $\leftarrow \emptyset$
System.gc()

using the exact algorithm in the *sGrapp* suit [25]. Figure 6(a) illustrates 8 young butterflies in an instance of W_{BG} (butterflies incident to j_0 are excluded):

$$\bowtie_{v_1} = \bowtie^{i_2,i_3}_{j_1,j_2}, \bowtie_{v_2} = \bowtie^{i_2,i_4}_{j_1,j_2}, \bowtie_{v_3} = \bowtie^{i_3,i_4}_{j_1,j_2}, \bowtie_{v_4} = \bowtie^{i_5,i_6}_{j_2,j_3}, \bowtie_{v_5} = \bowtie^{i_7,i_8}_{j_4,j_5}, \bowtie_{v_6} = \bowtie^{i_9,i_{10}}_{j_5,j_6}$$

$$\bowtie_{v_7} = \bowtie^{i_{11},i_{12}}_{j_6,j_7}, \bowtie_{v_8} = \bowtie^{i_{13},i_{14}}_{j_8,j_9}$$

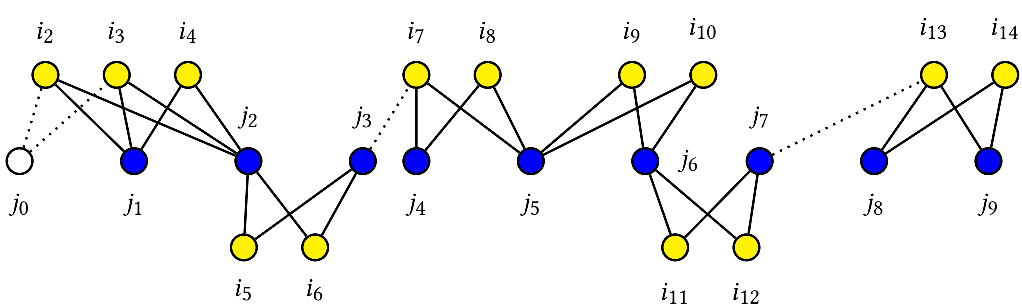

(a) BG snapshot. Young butterflies (solid lines) are connected through j-vertices.

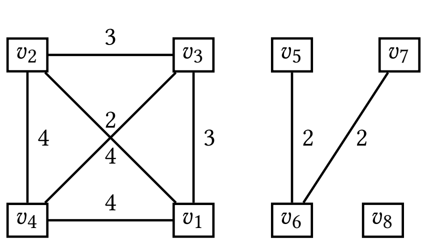

(b) Structure of UWGO

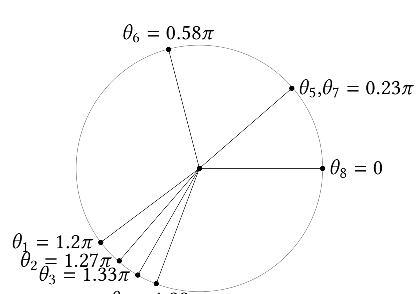

(c) Phases of UWGO vertices

Fig. 6. Projecting BG to $UWGO$.

For each young butterfly $\bowtie_v$, an oscillator vertex v is created with three attributes initialized to zero: phase, frequency, and identifier. The vertex identifier is then set to the hash code[3] of the object representing v and added to UWGO (Algorithm 4, lines 2-4). The cumulative butterfly count follows a power-law function of the total number of edges (*butterfly densification power-law* [25]), therefore we don't use an incremental number for the identifier. Instead we use a fixed-size ID and call the garbage collector afterward (Algorithm 4, line 9). v is connected to any existing vertex n whose corresponding young butterfly $\bowtie_n$ is in current W_{BG} and shares at least one j-vertex with $\bowtie_v$. Alternatively, connections can be based on shared i-vertices. The static weight of the edge between v and n is the number of butterflies adjacent to j-vertices of $\bowtie_v$ (Algorithm 4, Lines 5-7). Consequently, the UWGO vertices with higher weighted degrees represent the butterflies which are newer and connected to more and high degree butterflies. The reason is that W_{BG} vertices are stored and iterated in the data structures according to the order of their SGR ingestion/arrival. Therefore, butterflies whose elements are ingested later are identified later and their UWGO vertex is simultaneously connected to the previous ones with an edge weight equal to the number of its UWGO neighbours plus one. For example in Figure 6(b), v_1 and v_2 are connected by an edge with weight equal to 2 since $\bowtie_{v_2}$ is identified after $\bowtie_{v_1}$ and they share j_1 and j_2. Next, v_3 is connected to v_1 and v_2 with weight 3 and then, v_4 is connected to these three vertices with weight 4. v_6 connects to v_5, and v_7 connects to v_6 with weight 2.

2.b) The local data structures are renewed and garbage collector is called (Algorithm 4, lines 8-9). Also, all of the SGRs in W_{BG} are retired to avoid redundant updates to the system state (Algorithm 3, line 17).

2.c) The attributes of UWGO vertices are updated (Algorithm 3, lines 18- 20). The frequency Ω_v is sampled from a normal distribution with mean equal to zero and the phase is set as $\theta_v = (\sum_{n \in N(v)} n.ID)\%2\pi$. The phase of an oscillator embeds the neighbourhood of the corresponding butterfly. Butterflies are the building blocks of the stream. Therefore, projecting W_{BG} to W_{UWGO} implies embedding the stream to a latent space of phases in $[0, 2\pi)$. In Figure 6(c), $\theta_8 = 0$ since $\bowtie_{v_8}$ is not connected to other butterflies, $\theta_5 = \theta_7$ since $\bowtie_{v_5}$ and $\bowtie_{v_7}$ have one shared neighbour $\bowtie_{v_6}$, and the rest of the vertices except v_6 have close phases due to similar neighbourhoods.

A.2 SGDD - Drift Detection

The sequential procedures of drift criteria and drift evaluation are as the following (steps 3-6 and yellow boxes in Figure 5).

Drift Criteria. A common measure of the level of global phase synchronization in a network of phase oscillators is a quantity called order parameter [22]. We calculate it for sequential instances W of W_{UWGO} with oscillators V as the following.

$$O[W] = ((\sum_{v \in V} \sin\theta_v)^2 + (\sum_{v \in V} \cos\theta_v)^2)^{\frac{1}{2}} / |V|$$

$0 \leq O[W] \leq 1$, the higher $O[W]$, the greater the degree of synchronization. $O[W] = 1$ denotes a phase synchrony state where all vertices have the same phase, which means butterflies have similar neighbourhoods and are densely connected to each other. Two time-series, O_1 and O_2, as the drift criteria are recorded over time:

3) The order parameter is first computed over $UWGO$'s structure and phases as $O_1[W]$ (Algorithm 3, line 22). The phases in Figure 6(c) would result in $O_1 = 0.17$.

4) Kuramoto model [22] is the most popular approach to formulate the synchronization process in a population of interacting oscillators. It quantifies the phase change for each oscillator, according to its frequency and the significance of phase difference with its neighbours, such that a global synchronization can be reached. Given the current phases $\Theta = \{\theta_v\}$, edge weights $\{w_{vn}\}$, and frequencies $\{\Omega_v\}$, the phase evolution of a vertex v is denoted as $\frac{d\theta_v}{dt} = \Omega_v + \sum_{n \in N(v)} w_{vn} sin(\theta_v - \theta_n)$. This ordinary differential equation

[3]The Java method hashCode() must consistently return the same integer for 'equal' objects during one execution of a Java application. This method is not required to return distinct integers for unequal objects by general contract indicated in https://docs.oracle.com/. As much as is reasonably practical, the hashCode method defined by class Object does return distinct integers for distinct objects. Since the UWGO vertex objects are unequal, there is a probability for mapping different vertices to the same ID.

is solved using the Runge Kutta method with $h = 0.01$ (Algorithm 3, line 23).

$$\Delta\theta_v = \frac{h}{6}(K(1)_v + 2K(2)_v + 2K(3)_v + K(4)_v)$$

$$K(1)_v = \Omega_v + \Sigma_{n\in N(v)} w_{vn} \sin(\theta_n - \theta_v)$$

$$K(2)_v = \Omega_v + \Sigma_{n\in N(v)} w_{vn} \sin(\theta_n + \frac{h}{2}K(1)_n - \theta_v - \frac{h}{2}K(1)_v)$$

$$K(3)_v = \Omega_v + \Sigma_{n\in N(v)} w_{vn} \sin(\theta_n + \frac{h}{2}K(2)_n - \theta_v - \frac{h}{2}K(2)_v)$$

$$K(4)_v = \Omega_v + \Sigma_{n\in N(v)} w_{vn} \sin(\theta_n + hK(3)_n - \theta_v - hK(3)_v)$$

The model results in the following phases in Figure 6: $\Delta\theta_1 = 0.13$, $\Delta\theta_2 = 0.01$, $\Delta\theta_3 = -0.02$, $\Delta\theta_4 = -0.09$, $\Delta\theta_5 = 0.01$, $\Delta\theta_6 = -0.1$, $\Delta\theta_7 = 0$, $\Delta\theta_8 = 0.01$.

5) The order parameter is computed as $O_2[W]$ for predicted phase changes $\Delta\theta$ (Algorithm 3, line 24). The oscillators in the running example have $O_2 = 0.98$.

Drift Evaluation. The evolutions in O_1 and O_2 are evaluated to detect a CD (Algorithm 3, line 25).

6) A CD is signaled when the butterfly neighbourhoods are stable, while some butterflies display a future change in their neighbourhoods. Precisely, a drift is signaled when three conditions C_1, C_2, and C_3 are satisfied (Algorithm 5).

C_1: a local maximum/minimum is observed in O_2.
C_2: O_1 remains steadily fixed.
C_3: The last CD signal has been in at least 10 windows back.

C_1 is implemented as $(10^\alpha\mu_1 - 10^\alpha O_1[t])/10^\alpha < 10^{-\alpha}$, where μ_1 is the average of the last S' values of O_1 and α is a dynamic value used as a threshold and a precision for difference of μ_1 and $O_1[t]$.

C_2 is implemented as ($Ngreater \geq S'$ OR $Nless \geq S'$), where S' is a fraction of S and $Ngreater$ and $Nless$ denote the number of elements in the most recent suffix of S elements in O_2 that are greater and less than $O_2[t]$, respectively.

When a drift occurs, the structure of streaming graph perturbs and O_1 and O_2 experience frequent fluctuations, therefore C_1 and C_2 should adapt to these perturbations through proper setting of S, S', and α. This is to reach a balanced detection state between sensitivity and robustness.

- S is determined based on a function of the number of detections, average burst size, and maximum seen burst size (Algorithm 5, line 3). S fluctuates with changing of burst sizes. when S decreases, μ_1, $Ngreater$, and $Nless$ are computed over smaller suffix to pass the fluctuated values.
- S' decreases as the number of detections increases to ease C_2 and avoid missing drifts.
- α is calculated as the current number of detections plus two; therefore, as detections increase, C_1 gets more difficult to avoid false detections.

Algorithm 5: CD Check via Butterflies Interconnections

Function $CDC_{Butterfly}(\bar{B}, maxB, O_1, O_2, t, W, W_d serie)$

- $d \leftarrow W_d serie.size()$
- $S \leftarrow \frac{\lfloor log_{10}(Max(maxB,100)) \rfloor}{\lfloor log_{10}(Max(\bar{B},10)) \rfloor}^{(-1)^{d+1}}$
- $S' \leftarrow (1-d)S$
- $\mu_1 \leftarrow$ mean of the last S' values in O_1
- $Nmore \leftarrow$ number of elements among the last S elements of O_2 which are greater than $O_2[W]$
- $Nless \leftarrow$ number of elements among the last S elements of O_2 which are less than $O_2[W]$
- $\alpha \leftarrow d + 2$
- **if** $(Nless \geq S' \vee Nmore \geq S') \bigwedge (|[(10^{\alpha}\mu_1 - 10^{\alpha}O_1[k])]|/10^{\alpha}) < 10^{-\alpha}) \bigwedge W - W_d serie.lastElement() > 10$ **then**
  - Signal a drift at sgr index t, window W, and current system time
  - $W_d serie.add(W)$

Table 3. The average system time distance (ms) / SGR count distance of the ith CD and its first and last *SGDP*'s signals with suffix size determined as $S \leftarrow \frac{\lfloor log_{10}(Max(maxB,100)) \rfloor}{\lfloor log_{10}(Max(\bar{B},10) \rfloor})^{(-1)^d}$.

ms/sgr	d_{1f}	d_{1l}	d_{2f}	d_{2l}	d_{3f}	d_{3l}	d_{4f}	d_{4l}	d_{5f}	d_{5l}
G_{11}	621.21/990	0.5/433	2863.61/198998	110.42/6914	2374.17/96837	6.06/16592	36.08/91028	5.5415029	94.71/14290	11432.39/572992
G_{12}	544.56/990	0.54/433	2602.93/199064	0.79/1656	2273.68/89324	7.67/20581	39.92/97835	4.41/10190	4.7/10631	6619.2/516866
G_{13}	531.91/990	0.58/433	1553.38/199090	0.49/866	2576.25/92921	2.62/6921	40.05/96075	2.97/6728	1.56/3453	3853.21/588808
G_{14}	543.7/990	0.533/433	2256.41/199062	1.35/3372	1953.98/95679	635.61/6006	33.61/92278	1.48/3883	4.85/13423	3998.81/569089
G_{15}	525.28/990	0.61/433	3352.88/199126	2.74/7084	3128.61/98075	4.47/12774	34.06/89358	6.05/15611	2.05/5641	4326.21/530006
G_{21}	1327.35/982	0.49/433			832.89/16152	169.31/4558	25834.85/198742	83.8/638	157.41/1843	25650.69/397538
G_{22}	519.58/990	0.48/433	2551.06/199382	0.57/1096	2589.36/185393	8.26/24384	75.53/194324	5.8/14140	5.7/12664	3187.11/394536
G_{23}	574.21/990	0.56/433	3118.22/199220	1.12/3069	5497.82/184920	5.55/16546	58.85/179858	1.47/3710	25.7/68088	377.27/359944
G_{24}	522.79/990	0.5/433	2907.32/199156	0.3/733	3199.19/184041	636.2/36446	74.45/196190	7.2/17563	6.22/15330	3290.17/349942
G_{25}	523/990	0.48/433	3053.84/199001	0.78/1652	1552.73/181108	17.18/49227	73.49/198918	10.45/25915	1.7/4192	3981.72/307993
AVG	623.3/989.2	0.5/433	2695.5/199122.1	13.2/2938	2597.9/122445	149.3/19403.5	2630.1/143460.6	12.9/11340.7	30.5/14955.5	6671.7/458771.4

ms/sgr	d_{1f}	d_{1l}	d_{2f}	d_{2l}	d_{3f}	d_{3l}	d_{4f}	d_{4l}
R_{11}	552.8/990	0.5/433	2366.4/199007	1.82/4682	606.01/92643	11.05/27346	0.28/468	291.62/683795
R_{12}	527.08/990	0.44/433	2315.66/199004	1.4/3177	940/93872	1.35/3458	3.29/9926	268.4/685600
R_{13}	505.67/990	0.45/433	2497.91/199159	2.99/6894	3930.04/99564	6.09/18604	1.61/4433	274.23/698234
R_{14}	526.19/990	0.43/433	2616.27/199090	1.32/3252	3397.48/92309	3.81/10564	2.94/8373	276.94/691594
R_{15}	503.83/990	0.43/433	3592.33/199040	1.63/4427	2384.35/85237	944.28/11098	5.16/16380	243.57/670088
R_{21}	633.1/990	0.49/433	4665.46/399216	5.1/13644	6762.54/195310	20.54/56107	1.75/3939	145.13/369707
R_{22}	601.17/990	0.56/433	3424.14/399050	0.4/896	6018.52/184303	9.72/26277	2.68/6651	167.59/398792
R_{23}	557.2/990	0.55/433	3424.61/399183	2.59/7105	3534.66/192765	5.52/16287	4.02/11450	162.62/389676
R_{24}	550.89/990	0.48/433	2609.36/399183	0.46/1053	3588.61/189434	5.58/13771	2.52/6104	174.47/390063
R_{25}	522.73/990	0.5/433	3695.39/399188	3.15/8308	3286.01/195456	1.92/5126	5.61/16303	157.09/380914
AVG	548.1/990	0.5 /433	3120.7/310222	2.1/5416.8	3444.8/142089.3	101/18863.8	3/8402.7	216.2/535846.3